THE UNIVERSITY OF

WARWICK

University of Warwick institutional repository: http://go.warwick.ac.uk/wrap

This paper is made available online in accordance with
publisher policies. Please scroll down to view the document
itself. Please refer to the repository record for this item and our
policy information available from the repository home page for
further information.

To see the final version of this paper please visit the publisher's website.
Access to the published version may require a subscription.

The local adsorption site of methylthiolate on Au(111): bridge or atop?

D.C. Jackson, A. Chaudhuri, T.J. Lerotholi, D.P. Woodruff[*]

Physics Department, University of Warwick, Coventry CV4 7AL, UK

Robert G. Jones

School of Chemistry, University of Nottingham, Nottingham NG7 2RD, UK

V.R. Dhanak

Surface Science Research Centre, University of Liverpool and Daresbury Laboratory,

Warrington WA4 4AD, UK

Abstract

Measurements of the local adsorption geometry of the S headgroup atom in the Au(111)($\sqrt{3}$x$\sqrt{3}$)R30°-CH$_3$S surface have been made using normal incidence X-ray standing waves (NIXSW) and S 1s scanned-energy mode photoelectron diffraction on the same surface preparations. The results confirm that the local adsorption site is atop an Au atom in a bulk-continuation site with a S-Au bondlength of 2.42±0.02 Å, and that there can be no significant fraction of coadsorbed bridging species as recently proposed in a combined molecular dynamics/experimental study by Mazzarello *et al.* (Phys. Rev. Lett., 98 (2007) 016102). The results do not, however, clearly distinguish the different local reconstruction (adatom) models proposed for this surface.

keywords: photoelectron diffraction; X-ray standing waves; chemisorption; self-assembly; gold; thiols

[*] corresponding author, email D.P.Woodruff@warwick.ac.uk

1. Introduction

Despite the many investigations of alkylthiolates ($CH_3(CH_2)_{n-1}S$) adsorbed on Au(111) to produce so-called self-assembled monolayers (SAMs) (e.g. [1, 2, 3, 4]), motivated by a range of areas of technological application, the structure of the thiolate/metal interface remains in doubt. Of the limited number of investigations directed to solving this structural problem, the majority have focussed on the simplest system, namely that of methylthiolate (n=1). In particular, this adsorbate is not only open to study experimentally, but is also most amenable to investigation by theoretical total energy calculations that commonly fail to describe the weak but important dispersion forces that govern interactions of the longer (n>1) alkyl chains. Until recently however, there appears to have been a fundamental disagreement between the results of theoretical and experimental studies of this system, specifically for the most widely-studied Au(111)($\sqrt{3}$x$\sqrt{3}$)R30º-CH_3S phase which occurs at a nominal coverage of 0.33 ML. A large number of total-energy calculations of this phase, mainly based on density functional theory (DFT), have concluded that the S head-group atom occupies either a three-fold coordinated hollow site [5, 6, 7, 8], or a two-fold coordinated bridging site [9, 10, 11, 12], with some studies suggesting the S is displaced from the fully-symmetric bridge site towards the adjacent hollow [13, 14]. By contrast, two independent experimental studies, using entirely different experimental methods (S 2p photoelectron diffraction [15] and S 1s ionisation in normal-incidence X-ray standing waves (NIXSW) [16]), have concluded that the S atom occupies atop sites.

One possible solution to this conflict is that the great majority of the theoretical studies have, until very recently, considered only adsorption on an unreconstructed surface and, as such, may have failed to investigate the correct structural model. In fact the one early theoretical investigation that did consider some models involving surface reconstruction [12] did find one of these reconstruction models to have the lowest energy, although the favoured local adsorption geometry of the S atom was also bridging two surface Au atoms in bulk-continuation sites. More recently, specific reconstruction models (Fig. 1)

have emerged from two experimental studies. Scanning tunnelling microscope (STM) images at very low coverages have been interpreted in terms of the bonding of pairs of methylthiolate species to single Au adatoms to produce Au-adatom-dithiolate surface moieties [17]. The Au adatom is believed to occupy a bridging site on the underlying Au(111) surface with the S head-group atoms of the thiolate bonded to either side of this adatom such that they lie atop Au atoms in the underlying surface. The local ordering of this Au-adatom-dithiolate species, even at low coverages, is proposed to be consistent with the behaviour of long-chain alkylthiolates on Au(111) at low coverages when the alky chains are found to 'lie-down' on the surface. A rather different model has emerged from NIXSW studies of longer-chain alkylthiolates at high (0.33 ML) coverage (when the alkyl chains 'stand up' on the surface) [18], with Au adatoms in different three-fold coordinated hollow sites. For the specific case of the Au(111)($\sqrt{3}$x$\sqrt{3}$)R30º-CH_3S phase, however, this model comprises Au adatoms in bulk-continuation sites ('fcc hollows') with the S head-group atoms of a single methylthiolate atop this adatom. An important feature of both of these adatom reconstruction models is that the S head-group atoms of the thiolate are locally atop Au atoms in bulk-continuation sites. As such, both models of this adsorbate phase could be consistent with previously published experimental data from photoelectron diffraction and NIXSW. Total energy calculations provide some support for both models [17, 19, 20], although they appear to favour the Au-adatom-dithiolate model after taking account of the energy cost of creating the Au adatom.

However, most recently, a new combined experimental and theoretical study of the Au(111)($\sqrt{3}$x$\sqrt{3}$)R30º-CH_3S phase [21] has concluded that this structure actually involves co-occupation of Au-adatom-dithiolate moieties and thiolate species bonded directly to the underlying surface with the S head-group atoms in bridging sites. This structural model, involving quite a high degree of disorder, was obtained from molecular dynamics calculations, but found to give, with some modification, satisfactory fits to experimental data obtained from S 2p photoelectron diffraction and surface X-ray diffraction (SXRD). A specific finding of this study is that the relative coverage of Au-adatom-dithiolate moieties and bridging thiolate species is 1:1, implying that 2/3 of the S head-group atoms occupy local atop sites while 1/3 occupy bridging sites. The idea that there is a significant

degree of bridge site occupation is broadly consistent with the results of many of the earlier theoretical total energy calculations, yet this appears to be inconsistent with earlier experimental studies. However, the possibility of co-occupation of local bridge and atop sites was not considered explicitly in these earlier experimental studies and warrants further evaluation.

Here we present the results of new experiments in which both S 1s photoelectron diffraction and NIXSW measurements have been made on the same surface preparations. The use of the S 1s, rather than S 2p, for the photoelectron diffraction means that we require closely similar photon energies, and can therefore do all the experiments using the same synchrotron radiation beamline and thus on the same surface preparations, ensuring optimum comparability. We regard this as particularly important in view of the recent conclusion of Mazzarello *et al.* [21] that this surface has a high degree of disorder; under these circumstances, it is certainly possible that the exact degree of order is sensitive to the method of preparation, so comparing the results of different experiments on differently-prepared surface could be misleading. Notice, though, that both NIXSW and PhD probe the local structure of the S headgroup atom, so variations in *long-range* order have no direct influence on these measurements, *although* changes in short-range order, including the relative occupation of different coexisting adsorption geometries will be detected by these techniques. We show that these new data are consistent with earlier independent measurements by these two techniques which clearly identify the local S headgroup site as atop an Au atom in a bulk-continuation site, and are not consistent with a significant degree of occupation of local bridging sites.

2. Experimental Details

The experiments were conducted on the double crystal monochromator beamline 4.2 of the Synchrotron Radiation Source (SRS) at the CLRC's (Central Laboratories for the Research Councils) Daresbury Laboratory. This beamline has been described in detail elsewhere [22, 23, 24]; it is fitted with a pair of InSb(111) Bragg reflectors and a surface science end-chamber equipped with the usual *in situ* sample preparation and

characterisation facilities. A concentric hemispherical analyser (with the axis of the entrance lens at 40° to the incident photon beam in the horizontal plane) was used to measure the energy distribution curves (EDCs) of photoemitted electrons at fixed pass energy. The Au(111) crystal sample was cleaned *in situ* by the usual combination of argon ion bombardment and annealing cycles to produce a clean well-ordered $(22 \times \sqrt{3})$rect. 'herring-bone' reconstructed surface as assessed by the synchrotron radiation X-ray photoelectron spectroscopy (XPS) Auger electron spectroscopy and LEED. The methylthiolate surface phase was formed by exposures in the range 8-20 × 10^{-6} mbar s of dimethyldisulphide (CH_3S-SCH_3) vapour with the sample at room temperature. S 1s XPS measurements showed these exposures led to saturation coverage, whilst LEED showed the expected $(\sqrt{3} \times \sqrt{3})R30°$ pattern. Notice that this LEED pattern clearly indicates that the thiolate lifts the original reconstruction of the clean Au(111) surface, an effect also seen at much lower coverages by STM (e.g. [17]). The electron beam in LEED is known to cause significant radiation damage to this surface, so having established the procedure for forming the surface, LEED observations were limited to checks after data collection. Indeed, an intense synchrotron radiation beam can also cause damage to this surface, and we have observed this effect on a far more intense undulator beamline at the European Synchrotron Radiation Facility in Grenoble [25], but with weaker focussing and a bending magnet source at the SRS there was no evidence of desorption or dissociation (as monitored by XPS) in the present experiments.

Two distinctly different experiments were performed on each surface preparation, namely NIXSW and scanned-energy mode photoelectron diffraction (PhD). In NIXSW [26, 27] an X-ray Bragg reflection is established in the underlying crystal through interference of the incident and Bragg-reflected waves. The location of the adsorbate atoms in the X-ray standing wavefield is then determined by measuring the variation in the X-ray absorption at the adsorbate atom as the X-ray energy is varied, and the standing wavefield sweeps through the adsorbate atom. This allows one to obtain quantitative information on the location of the adsorbate atoms relative to the underlying substrate. In the present study NIXSW measurements were made at normal incidence to the (111) scatterer planes, parallel to the surface, to provide a measure of the height of the sulphur headgroup atom

above the surface, and at normal incidence to the $(\bar{1}11)$ scatterer planes, to determine, by triangulation, the lateral position of the sulphur atoms, and hence their adsorption site. The relative absorption at the S atoms was monitored by measuring the intensity of the S 1s photoemission peak as a function of photon energy through the narrow energy range around ~2640 eV corresponding to the {111} normal incidence Bragg condition. These experimental NIXSW profiles were analysed according to our standard procedures to extract the two associated structural parameters [26, 27, 28], namely the coherent position d_H (where H specifies the Miller indices of the scatterer planes) and the coherent fraction f_{co}. In the simplest case of an absorber occupying a single well-defined site, d_H is equal to the perpendicular distance of this site from the scattering planes, while f_{co} is a measure of the degree of local order, a value of unity implying perfect (static and dynamic) order. Low values of f_{co} (much smaller than that for the substrate) typically imply two or more coexistent local adsorption geometries.

The PhD technique [29, 30] exploits the coherent interference of the directly-emitted component of the outgoing photoelectron wavefield from a core level of an adsorbate atom with components of the same wavefield which are elastically backscattered by the nearby substrate atoms. By measuring the photoemission intensity in specific directions as a function of photon energy, the resulting changes in photoelectron energy, and thus photoelectron wavelength, cause specific scattering paths to switch in and out of phase with the directly-emitted component, leading to modulations in the intensity which depend on the relative emitter-scatterer location. Simulations of these PhD modulation spectra, including multiple scattering from the surrounding atoms in 'guessed' model structures, allow one to determine the local adsorption geometry by adjusting the model structure to optimise the theory-experiment agreement. The present measurements focussed on the S 1s PhD at normal emission. A similar measurement was also made at a polar emission angle of 55°, but showed only very weak modulations; while weak modulations are to be expected in this geometry for an atop emitter site, the poor signal-to-noise ratio of this spectrum means it is unsuitable for quantitative modelling. A PhD data set restricted to a single (normal) emission direction is not really adequate for a complete structure determination of an unknown system, but can provide very specific

quantitative information on the optimised geometry of alternative structural models. An important distinction between the NIXSW and PhD methods is that while NIXSW locates the absorber atom relative to the underlying bulk, PhD allows one to obtain quantitative information on the location of the near-neighbour substrate atoms. These two complementary pieces of information prove to be of considerable value in the present investigation.

The basic experimental strategy for data collection in the NIXSW and PhD studies was actually very similar: in both cases a sequence of S 1s photoelectron energy distribution curves (EDCs) was collected in a fixed geometry at regular steps in photon energy. In the case of the NIXSW experiment, the photon energy step size is small (0.2 eV), and the energy range is narrow (~10 eV), centred around the energy of the Bragg condition, the key geometrical consideration being the incidence direction (normal to the scatterer planes). For the PhD experiment the photon energy step size and range are larger (4 eV and ~200 eV respectively), and it is the detected emission direction that is of primary importance. In both experiments the integrated intensities of the S 1s peak, obtained by fitting the individual EDCs to a Gaussian peak and a background, were then plotted as a function of photon energy. The resulting normalised modulation spectra form the basis of the subsequent structure determination by the two methods.

As the two measurements included measurements of the S 1s photoemission intensity in an overlapping photon energy range, it is perhaps appropriate to comment on the possible interference of the two phenomena in the resulting data. For the PhD measurements, the incident geometry was always far from a normal incidence standing wave condition; under these conditions the mosaicity of a standard metal single crystal ensures that no significant standing wave effects are seen. For the NIXSW measurements, PhD modulations must, in principle, overlap those due to the standing wave. However, not only are the NIXSW modulations typically substantially larger than those of PhD, but the (local) energy period of the NIXSW modulation is also very much narrower than that due to PhD (typically ~3 eV compared with 30 eV), so the effect of any PhD modulation is just to introduce a slight slope to the background of the NIXSW modulation spectrum.

7

One problem common to both measurements of S on Au(111), however, is the influence of Au Auger electron emission peaks in the kinetic energy range around 140-160 eV; as the photon energy varies and the S 1s photoemission peak passes over these substrate emission features, reliable separation proves difficult. In the case of the PhD data, the unreliability of this separation led to a reduced kinetic energy range from 167 eV to 323 eV being used in the structure analysis. The enhanced modulation amplitude and reduced energy range of the NIXSW modulation means the problem is slightly less severe for this technique, but it does lead to some spurious distortion of the data on the low energy side of the standing wave profile due to a substrate Auger emission peak around 144 eV, as discussed previously [16].

3. Results
3.1 NIXSW

NIXSW measurements of the Au(111)($\sqrt{3}$x$\sqrt{3}$)R30°-CH$_3$S phase have been reported in the past [16] and the new results are in good agreement with these previous measurements. Fig. 2 shows one set of experimental (111) and ($\bar{1}$11) S NIXSW absorption profiles from this surface recorded at room temperature, superimposed on the theoretical simulations using the best-fit values of the coherent position and coherent fraction. Note that the discrepancy between theory and experiment at the lowest energies is due to the problem of the overlapping S 1s photoemission and Au Auger peaks discussed in the previous section. The fitting parameter values, based on two measurements of this surface preparation the fitting parameter values, are listed in Table 1. Included in this table are the corresponding values for absorption in the Au substrate atoms, obtained from fitting the absorption profile given by the inelastically-scattered electron background signal of the S 1s photoemission. For an ideally bulk-terminated substrate, the value of $d_{(111)}$, expressed in units of the Au(111) bulk interlayer spacing, is expected to be 1.00, but seems to be consistently slightly smaller than this, possibly indicating some relaxation of the outermost layer spacings of the adsorbate-covered, and probably reconstructed, Au surface. The fact that the Au $d_{(-111)}$ value is closer to unity would be consistent with the Au atom displacement being perpendicular to the surface, as

8

siple triangulation shows that the effect of such a displacement would be a factor of three smaller on $d_{(-111)}$ than on $d_{(111)}$. For S absorption, the $d_{(111)}$ value of Table 1 corresponds to a height of the S atom above the outermost Au layer for an unrelaxed surface of $z = 2.44\pm0.07$ Å, in excellent agreement with the previously published value of 2.48±0.05 Å [16]. Notice that the NIXSW technique measures the distance of the S atom relative to the extended bulk scatterer planes, so if there is relaxation of the outermost interlayer spacings this value may not correspond to the true nearest-neighbour S-Au interlayer spacing, but would have to be corrected for this net relaxation. The high value of $f_{(111)}$ (quite close to the maximum possible value of unity) strongly suggests that all S atoms are at the same height above the surface. The value of $d_{(-111)}$, also in agreement with the earlier reported value, shows that the S atom occupies an atop site relative to the underlying Au solid. In particular, the expected values of $d_{(-111)}$ for occupation of the three high-symmetry adsorption sites of atop, hcp hollow (above a second layer Au atoms) and fcc hollow (above a third layer Au atoms) are, respectively, $(d_{(111)}/3)$, $(d_{(111)}/3) + 0.33$, and $(d_{(111)}/3) + 0.66$, and the corresponding numerical values are given in Table 2. The experimental value of 0.34±0.03 matches well the predicted value for the atop site of 0.35. The ;$f_{(-111)}$ value is also similar to (but slightly higher than) that of the earlier report, indicating a good degree of local order. Note that the bridge site leads to predicted $d_{(-111)}$ and $f_{(-111)}$ values that are clearly incompatible with the experimental results.

While these measurements confirm the earlier NIXSW results, they also form an important dataset with which to compare the results of the PhD measurements recorded from the same surfaces.

3.2 Photoelectron diffraction

As remarked earlier, the PhD technique provides a means of determining, in an entirely different fashion, the *local* S-Au coordination and bondlength. Two previous studies of the Au(111)($\sqrt{3}$x$\sqrt{3}$)R30º-CH$_3$S surface have included normal emission S PhD experiments, but both of these have used S 2p emission at lower photon energies but in

the same (but larger) photoelectron kinetic energy range. Our own measurements on the S 1s PhD spectra are not directly comparable, because the initial state angular momentum quantum number differs. However, it has previously been shown, in an investigation of K on Ni(111) [31]), that in such studies the PhD spectrum from an initial p-state is, to quite a good approximation, simply the negative of the PhD spectrum from an initial s-state (i.e. the sign of the modulation spectrum is inverted, switching maxima to minima and *vice versa*) . The reason for this is that the outgoing p-wave emitted from an initial s-state has odd parity, while the outgoing s- and d-waves emitted from an initial p-state both have even parity. In a typical experimental geometry this means that, relative to the directly emitted component of the photoelectron wavefield reaching the detector, there is a phase shift of π in most of the scattered components in the odd-parity outgoing wave that is not present in the even-parity outgoing wave. The conditions for constructive and destructive interference of the directly-emitted and scattered components are thus inverted for the two different initial states.

Fig. 3 shows a comparison of the negative of the S 1s PhD spectrum measured in the present study with the S 2p PhD spectra from the two previous studies [15, 21]. In both of these earlier investigations the modulation intensities were reported as a function of photoelectron wavevector, k, rather than energy, and Fig. 3 shows these data as shown in the original publications. Although these two S 2p spectra are qualitatively similar, there is an offset on the ordinate between them. This may be due in part to different values of the experimental contact potential difference, but may also be due to different assumptions regarding the inner potential prior to the energy-to-k conversion. It is not clear whether these authors have presented their data in terms of k values outside the crystal (at the measured energies) or inside the crystal (where the diffraction occurs). To accommodate these differences, we have applied adjustments to the measured kinetic energies on our S 1s spectra to achieve the best match of the modulations with each of the earlier studies. In order to match the spectrum of Kondoh *et al.* [15] an offset of 7.5 eV has been used; i.e. our experimental kinetic energies have been increased by 7.5 eV, consistent with assuming an inner potential of this value. To match the spectrum of Mazzarello *et al.* [21], on the other hand, a value of -5.5 eV was required. Notice that

these different values reflect a difference in the *k*-scale of the S 2p spectra in these two publications. A negative value of the inner potential is not, of course, physically meaningful, but it is possible that no inner potential correction was applied to these data in displaying the spectrum as a function of *k*, and that the small negative value is then attributable to contact potential effects. The exact value of this offset is also, of course, subject to some error in assessing how best to match the modulations of the 1s and 2p spectra. While our data range is significantly shorter than those of the S 2p measurements, due to a weaker signal and a resulting greater difficulty in separating the photoemission and Auger electron peaks, it is clear that the general periodicity and modulation amplitude is closely similar, as expected.

In order to determine the structure from the PhD data, multiple scattering simulations are performed for a range of trial structures. The calculations were performed with computer codes developed by Fritzsche [32, 33, 34] that are based on the expansion of the final state wave-function into a sum over all scattering pathways that the electron can take from the emitter atom to the detector outside the sample. For each structural model and set of structural parameter values a multiple scattering simulation of the selected experimental PhD spectra was performed and the quality of agreement between theory and experiment judged by the value of an objective reliability- or *R*-factor, defined as a normalised summation of the squares of the differences between the experimental and theoretical modulation amplitudes at each point in the spectra [29, 30]. Fig. 4 shows a comparison of the experimental S 1s PhD spectra (as measured as a function of photoelectron kinetic energy in the vacuum) and four different structural models, in each case with the value of the main structural parameter, the height of the S atom above the nearest-neighbour Au atoms, *z*, that best fits the experimental data. The bottom three spectra correspond to the different models in which the S atom lies atop an Au atom, namely atop out outermost layer Au atom in an unreconstructed surface, atop an Au adatom that occupies a bulk-continuation (fcc hollow) site, and atop an outermost layer Au atom but adjacent to a bridging Au adatom within an Au-adatom-dithiolate moiety. In each case the optimum value of the S-Au nearest-neighbour interlayer spacing, *z*, is 2.42±0.02 Å, the precision being determined from the variance of the *R*-factor. This is

identical to the value found by Kondoh *et al.* assuming an unreconstructed Au(111) surface, although rather different from the value of 2.49 Å quoted by Mazzarello *et al.* [21] in their optimisation of this structural model.

Also shown in Fig. 4 is a comparison of the experimental PhD spectrum with the best-fit model in which the S atom is assumed to occupy a bridge site midway between two surface Au atoms on an unreconstructed surface. A reasonable fit is achieved to this restricted data range at a value of z of 1.63 Å. The R-factor values for the four comparisons shown in Fig. 4 are: atop unreconstructed surface, 0.104; atop Au adatom, 0.071; atop in S-Au-S moiety, 0.127; bridge 0.116. The variance of the minimum value of the R-factor is 0.040, so formally we should reject all solutions for which R is greater that 0.071+0.040=0.101. This would imply that only the model involving S atop an fcc Au adatom is acceptable, but with such a short data range it would be dangerous to apply this criterion too rigorously. The real constraint on the data range is the lack of significant modulations in other emission geometries, and this is also a feature of the earlier data of Kondoh *et al.* who report modulations that are mostly less that ±10% at 60° polar emission angle. Fig. 4 shows that tolerable agreement is achieved for all four models, so not only do these data not provide a convincing basis for distinguishing the different local atop models, but even the bridge site cannot be reliably rejected. We should note, however, that this bridge site model, with a local layer spacing of 1.63 Å, corresponds to a S-Au nearest-neighbour bonding distance of only 2.17 Å, very much shorter that that found for the atop site (2.42 Å) and very much shorter than the values found in DFT calculations which fall, for different geometries, in the range ~2.38-2.67 Å [15]. Within this theoretical bondlength range Kondoh *et al.* found the lowest value of their R-factor for the bridge site occurred at a bondlength of 2.42 Å, but this value was a factor of three larger than the low value obtained for the atop site. Our own PhD theory/experiment comparison for a bridge site at this bondlength gives a value of $R = 1.54$; a value greater than unity implies anti-correlation of the experimental and theoretical spectra. Evidently, therefore, even a fractional occupation of a bridging site at this bondlength leads to an unacceptable degradation of the PhD theory/experiment fit. However, at least for the limited data range of our PhD data, some admixture of the S-Au-S moiety and the bridge

site with the shorter bondlength could prove acceptable, but with the S atoms in the two sites at very different layer spacings, namely 2.42 Å and 1.63 Å. As we show below, such a model is *not* compatible with the NIXSW data.

4. Discussion

Much the most obvious interpretation of the new experimental results presented in the previous section is that the S headgroup atom of methylthiolate in the (√3x√3) phase on Au(111) occupies sites atop a surface Au atom in a bulk continuation site. Data from both the NIXSW and PhD techniques clearly lead to this conclusion independently and the numerical values of height of the S atom above the surface obtained by the two methods are in excellent agreement. Exactly which of the three possible local atop-site models is correct is less clear. NIXSW is 'blind' to the exact location of the neighbouring Au atoms, and so offers no way to distinguish the models. The PhD data analysis favours the model in which the S atom lies atop an Au adatom in a (bulk-continuation) fcc hollow site, but the data range is too narrow to regard this result as conclusive.

The primary motivation for this investigation, however, was to evaluate the proposal of Mazzarello *et al.* [21] that there is significant co-occupation of atop sites (in Au-adatom-dithiolate moieties) and of bridging sites (the left-hand and central models of Fig. 1). The main evidence for this comes from the molecular dynamics calculations that find co-occupation of Au-adatom-dithiolate moieties and bridging thiolate species in the ratio 1:1, corresponding to a 2:1 ratio of occupation of S headgroup atoms in local atop and bridging sites. As discussed in section 3.2, our PhD data could be compatible with such a model if the S-Au interlayer spacings of the two sites are 2.42 Å and 1.63 Å. Such a model is not, however, compatible with the NIXSW data. In particular, it is straightforward to calculate the coherent position and fraction values for such a model [35]. The combination of these two interlayer spacings would lead to (111) NIXSW parameter values of 0.95 for the coherent position and a maximum possible value of 0.57 for the coherent fraction. This coherent fraction value assumes that there is no static or dynamic disorder in either of the two local geometries; in practice this value should be

reduced by 10-20%, so an expected value for the coherent fraction of 0.50 is a more realistic estimate. Neither value is consistent with the experimental values of $d_{(111)}$ = 1.04±0.03 and $f_{(111)}$ = 0.89±0.10. Note that if one assumes the bridging S atoms do not have the short Au-S bondlength in the bridging site associated with the interlayer spacing of 1.63 Å, but the same bondlength as in the atop site, the interlayer spacing for the bridge site increases to 1.94 Å, and the predicted (111) NIXSW parameter values become $d_{(111)}$ = 0.96 and $f_{(111)}$ ≈ 0.70, still well outside the experimental error estimates. Moreover, as remarked in section 3.2, this larger S-Au interlayer spacing for the bridge site is incompatible with the PhD data.

In truth, Mazzarello *et al.* also find that a substantial occupation of the bridging site is not favourable for their photoelectron diffraction data, with their best-fit solution having an occupation ratio of Au-adatom-dithiolate moieties to bridging thiolate species of 3:1, corresponding to a 6:1 ratio of occupation of local atop and bridging sites. They also report that even this modest level of 14% occupation of the bridging sites leads to a deterioration in the quality of fit to their PhD spectrum; they find some improvement in the fit to their angle-scan photoelectron diffraction data for this model relative to that of S atop an unreconstructed surface, but it is not clear if the bridge site occupation really contributes to this improvement. The other key piece of experimental data presented by Mazzarello *et al.* in their study was from surface X-ray diffraction measurements, but these data are primarily influenced by the much stronger scattering from the Au atoms (notably from the Au adatoms and from the influence of Au surface atom vacancies) and it seems that bridging S atoms have little influence on these data.

In summary, our combined NIXSW and PhD study of the same surface preparations of Au(111)(√3x√3)R30º-CH_3S confirm earlier findings that the S headgroup atom occupies a site atop Au atoms in bulk-continuation sites and specifically excludes a model involving co-occupation of local atop and bridging sites in the ratio found in a recent molecular dynamics calculation. Fractional occupation of bridging sites leads to worse theory/experiment agreement for both techniques but, within the estimated experimental precision, some small fractional bridge site occupation (at a much shorter S-Au nearest-

neighbour bondlength of ~2.17 Å) cannot be excluded; estimates based on the NIXSW parameters and their estimated precision, however, indicate this fraction occupation could be ≤10% .

Acknowledgements

Table 1. Summary of the NIXSW structural parameters obtained from the Au(111)($\sqrt{3}$x$\sqrt{3}$)R30°-CH$_3$S surface. The associated comparison of the experimental data and the fits based on these parameters for the S absorbed atoms are shown in fig. 2.

element	$d_{(111)}$	$f_{(111)}$	$d_{(-111)}$	$f_{(-111)}$
Au	0.96±0.02	0.84±0.02	0.99±0.02	0.82±0.03
S	1.04±0.03	0.89±0.10	0.34±0.03	0.77±0.10

Table 2. Comparison of the experimental values of the ($\bar{1}$11) NIXSW parameter values for S absorption (Table 1) with theoretical predictions based on triangulation of the experimental (111) NIXSW parameters for different adsorption sites. The predicted $f_{(-111)}$ values for the three fully-symmetric sites are estimates based on the other measured f values; that for the bridge site includes the reduction by a factor of 3 that is intrinsic to this triangulation.

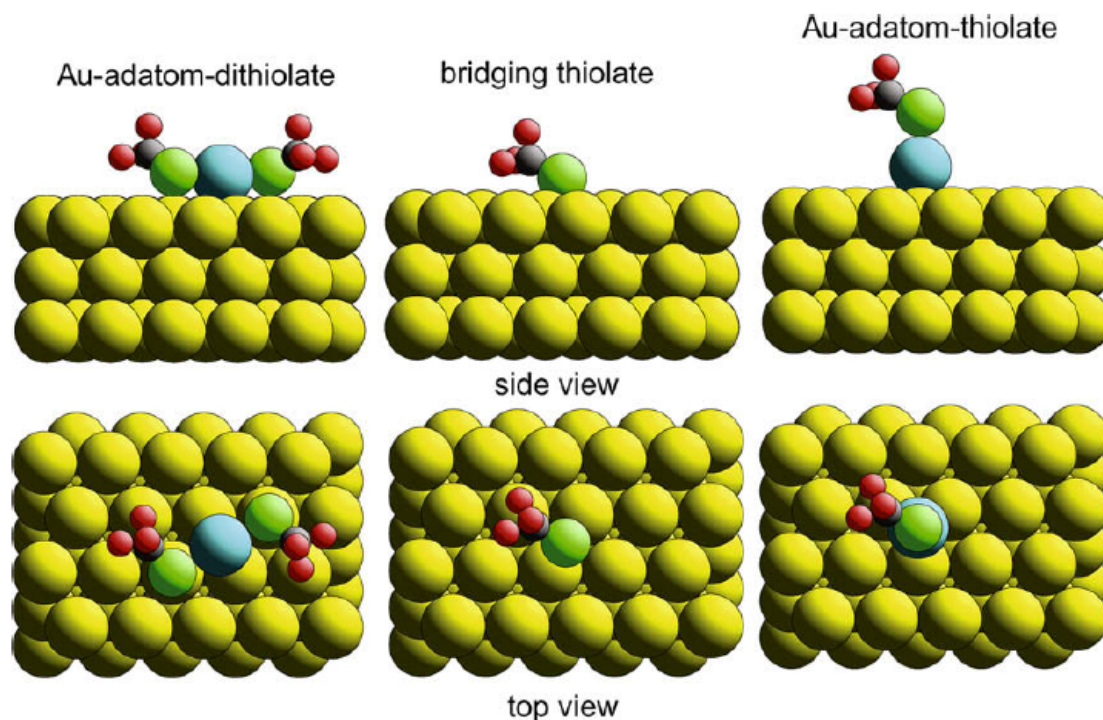| parameter	experiment	theory			
		atop	fcc hollow	hcp hollow	bridge
$d_{(-111)}$	0.34±0.03	0.35	0.01	0.68	0.85
$f_{(-111)}$	0.77±0.10	~0.80	~0.80	~0.80	~0.26

Figure Captions

Fig. 1 Schematic side views of the two recently-proposed Au adatom reconstruction models for the Au(111)/methylthiolate surface, and the bridging thiolate species on the unreconstructed surface. On the left is shown the Au-adatom-dithiolate model in which two thiolate species lie on either side of a bridge-bonded Au adatom with the S atoms in near-atop sites relative to the underlying Au(111) surface. On the right is shown the Au-adatom-thiolate model in which the thiolate lies atop an Au adatom which occupies a bulk-continuation fcc hollow site. In the centre is the simple bridging thiolate that has been proposed to coexist on the surface with the Au-adatom-dithiolate species.
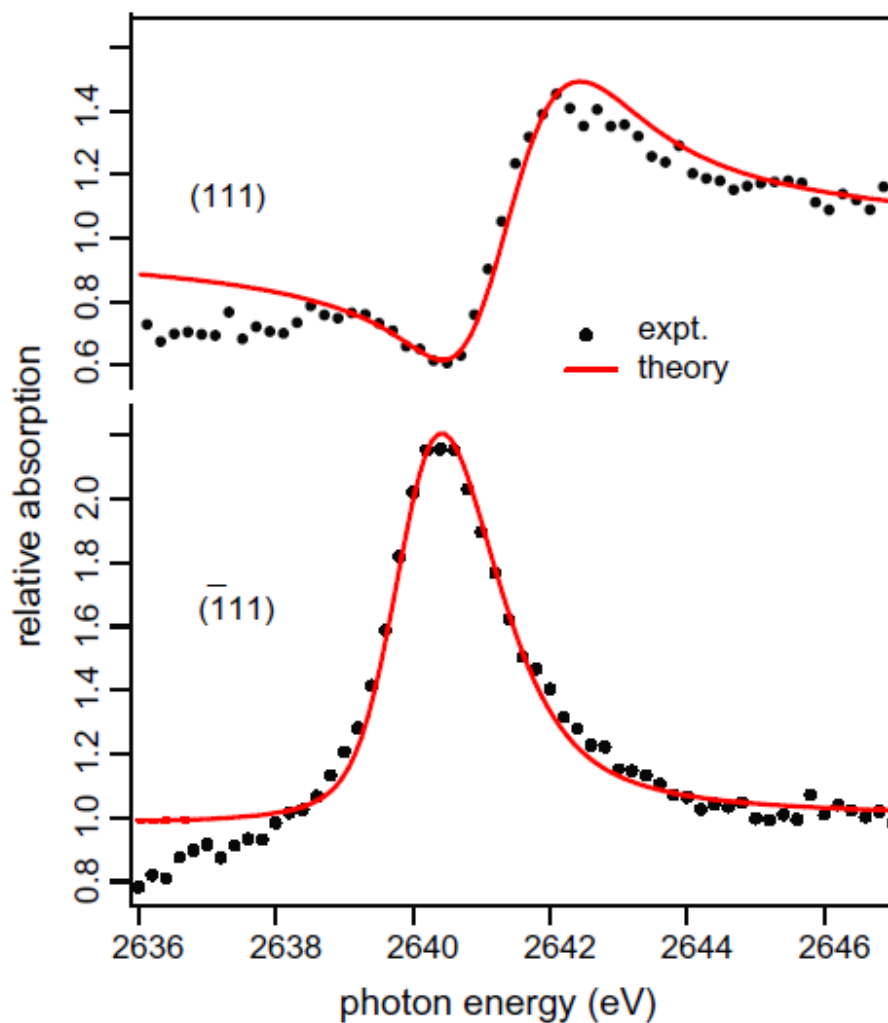
Fig. 2 Comparison of experimental (circles) and theoretical fits (full lines) NIXSW absorption profiles obtained at the S headgroup atoms of the Au(111)($\sqrt{3}$x$\sqrt{3}$)R30°-CH$_3$S surface.
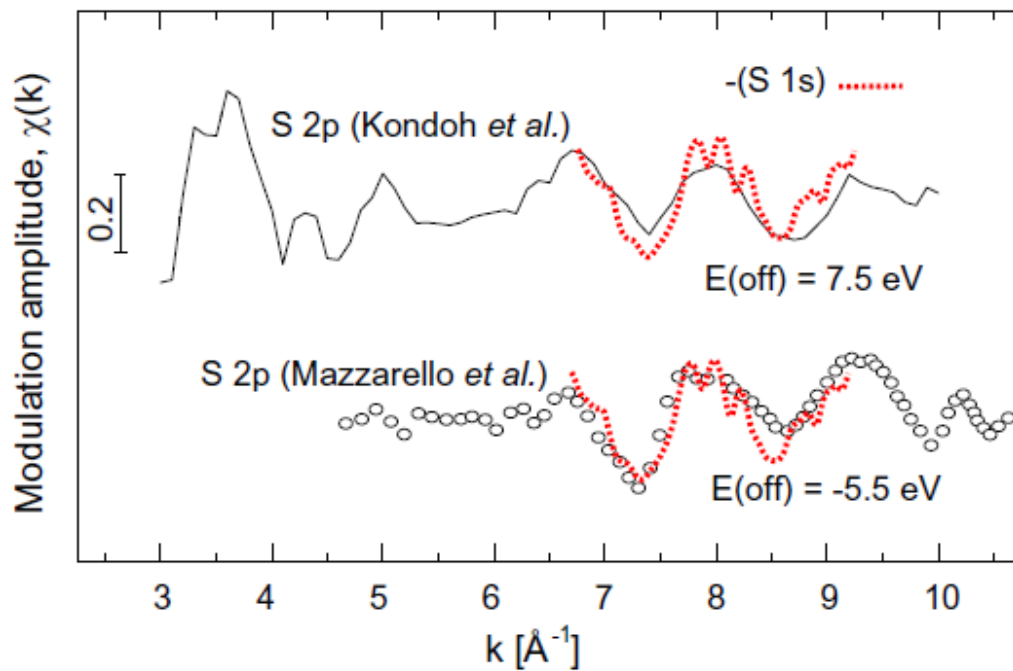
Fig. 3 Comparison of the previously-published S 2p normal emission PhD data from the Au(111)($\sqrt{3}$x$\sqrt{3}$)R30°-CH$_3$S surface, shown plotted (as in the original publications [15, 21]) as a function of electron wavevector, k, with the negative of the S 1s PhD spectrum obtained in the present work (see text). Different energy offset values for the new data to provide the best match to these earlier studies have been applied, as discussed in the text.
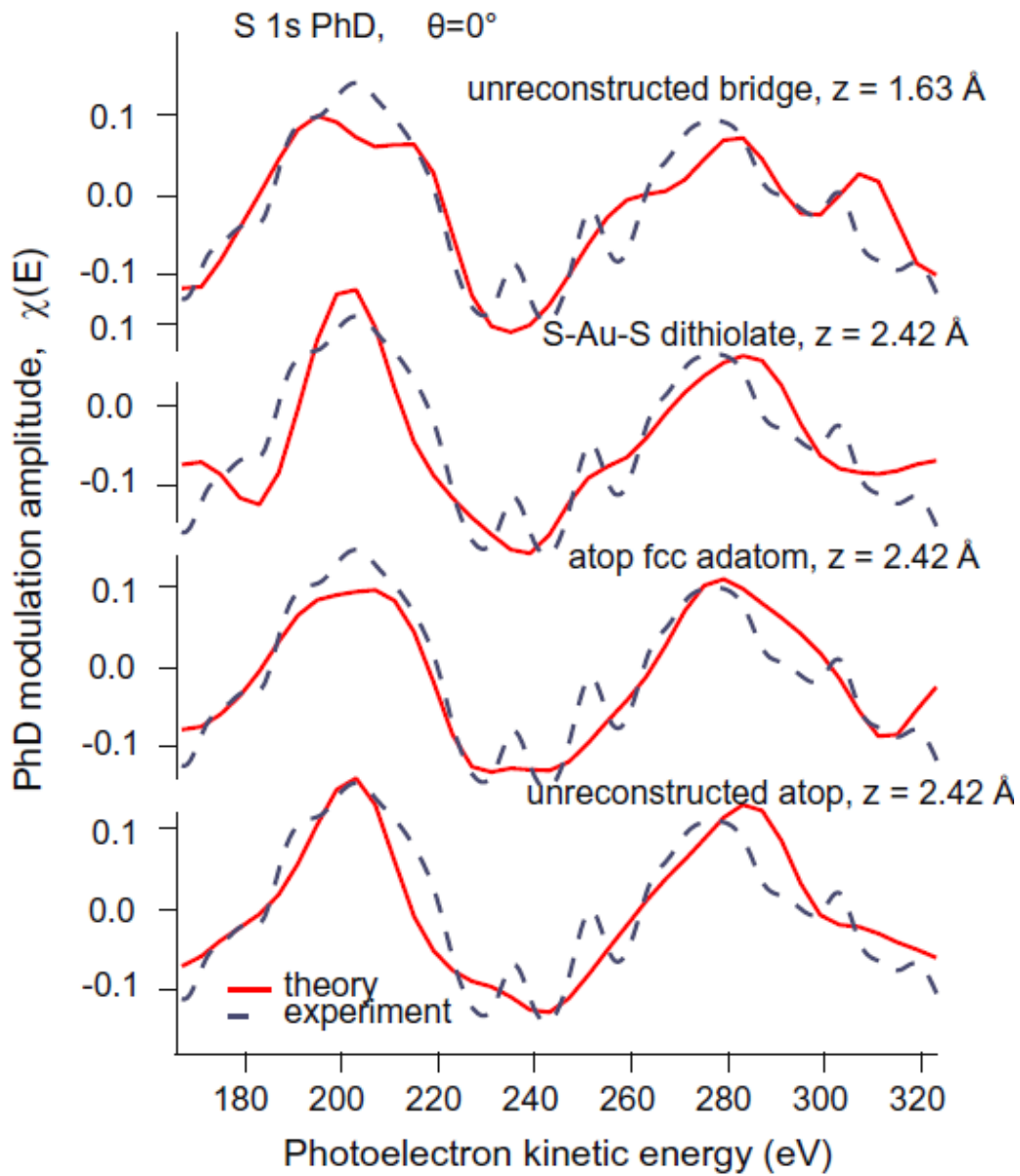
Fig. 4 Comparison of the experimental S 1s normal emission PhD data (dashed lines) from the Au(111)($\sqrt{3} \times \sqrt{3}$)R30°-CH$_3$S surface with the best-fit theoretical simulations (full lines) for different possible model structures, as discussed in the text.

References

1 L. H. Dubois, R. G. Nuzzo, Annu. Rev. Phys. Chem. 43 (1992) 437.

2 F. Schreiber, Prog. Surf. Sci. 65 (2000) 151.

3 A. Ulman, Chem. Rev. 96 (1996) 1533.

4 C. Vericat, M. E. Vela, R. C. Salvarezza, Phys. Chem. Chem. Phys. 7 (2005) 3258.

5 H. Sellers, A. Ulman, Y Shnidman, J.E. Eilers, J. Am. Chem. Soc., 115 (1993) 9389.

6 H. Gronbeck, A. Curioni, W. Andreoni, J. Am. Chem. Soc., 122 (2000) 3839.

7 Y. Yourdshahyan, H.K. Zhang, A.M. Rappe, Phys. Rev. B, 63 (2001) 081405.

8 M. Tachibana, K. Yoshizawa, A. Ogawa, H. Fujimoto, R. Hofmann, J. Phys. Chem. B, 106 (2002) 12727.

9 T. Hayashi, Y. Morikawa, H. Nozoye, J. Chem. Phys., 114 (2001) 7615.

10 M.C. Vargas, P. Giannozzi, A. Selloni, G. Scoles, J. Phys. Chem. B, 105 (2001) 9509.

11 J. Gottschalck, B. Hammer, J. Chem. Phys., 116 (2002) 784.

12 M.L. Molina, B. Hammer, Chem. Phys. Lett., 360 (2002) 264.

13 Y. Akinaga, T. Nakajima, K. Hirao, J. Chem. Phys., 114 (2001) 8555.

14 Y. Morikawa, T. Hayashi, C.C. Liew, H. Nozoye, Surf. Sci., 507-510 (2002) 46.

15 H. Kondoh, M. Iwasaki, T. Shimada, K. Amemiya, T. Yokohama, T. Ohta, M. Shimomura, K. Kono, Phys. Rev. Lett. 90 (2003) 066102.

16 M.G. Roper, M.P. Skegg, C.J. Fisher, J.J. Lee, V. R. Dhanak, D.P. Woodruff, R. G. Jones, Chem. Phys. Lett. 389 (2004) 87.

17 P. Maksymovych, D. S. Sorescu, J. T. Yates, Jr. Phys. Rev. Lett. 97 (2006) 146103.

18 Miao Yu, N. Bovet, Christopher J. Satterley, S. Bengió, Kevin R. J. Lovelock, P. K. Milligan, Robert G. Jones, D. P. Woodruff, V. Dhanak, Phys. Rev. Lett. 97 (2006) 166102.

19 F. P. Cometto, P. Paredes-Olivera, V. A. Macagno, E. M. Patrito, J. Phys. Chem. B 105 (2005) 21737.

20 H. Grönbeck and H. Häkkinen, J. Phys. Chem. B, 111 (2007) 3325.

21 R. Mazzarello, A. Cossaro, A. Verdini, R. Rousseau, L. Casalis, M.F. Danisman, L. Floreano, S. Scandolo, A. Morgante, G. Scoles, Phys. Rev. Lett., 98 (2007) 016102.

22 V.R. Dhanak, A.W. Robinson, G. van der Laan, G. Thornton, Rev. Sci. Instruments 63 (1992) 1342.

23 A.W. Robinson, S. D'Addato, V.R. Dhanak, P. Finetti, G. Thornton, Rev. Sci. Instruments 66 (1995) 1762.

24 Further information on the NIXSW station 4.2 at SRS Daresbury can be found at <http://www.srs.ac.uk/srs/stations/station4.2.htm>

25 A. Chaudhuri, M. Odelius, R.G. Jones, T.-L. Lee, B. Detlefs, D.P.Woodruff, submitted for publication.

26 D.P. Woodruff, Prog. Surf. Sci. 57 (1998) 1.

27 D.P. Woodruff, Rep. Prog. Phys. 68 (2005) 743.

28 The Igor routines of XSWfit can be obtained from robert.g.jones@nottingham.ac.uk.

29 D. P. Woodruff, A. M. Bradshaw, Rep. Prog. Phys. 57 (1994) 1029.

30 D. P. Woodruff, Surf. Sci. Rep. 62 (2007) 1.

31 V.Fritzsche, R.Davis, X.-M.Hu, D.P.Woodruff, K.-U.Weiss, R.Dippel, K.-M.Schindler, Ph.Hofmann and A.M.Bradshaw Phys. Rev. B 49 (1994) 7729.

32 V. Fritzsche, J. Phys.: Condens. Matter 2 (1990) 1413.

33 V. Fritzsche, Surf. Sci. 265 (1992) 187.

34 V. Fritzsche, Surf. Sci. 213 (1989) 648.

35 D.P. Woodruff, B.C.C. Cowie, A.R.H.F. Ettema, J. Phys. Condens. Matter 6 (1994) 10633.